New Phytologist

Research

Water uptake can occur through woody portions of roots and facilitates localized embolism repair in grapevine

Italo F. Cuneo[1], Thorsten Knipfer[2], Pratiti Mandal[3], Craig R. Brodersen[4] and Andrew J. McElrone[2,5]

[1]Escuela de Agronomía, Pontificia Universidad Católica de Valparaíso, Quillota 2260000, Chile; [2]Department of Viticulture and Enology, University of California, Davis, CA 95618, USA; [3]Advanced Light Source, Lawrence Berkeley Laboratory, Berkeley, CA 94720, USA; [4]School of Forestry & Environmental Studies, Yale University, New Haven, CT 06511, USA; [5]Crops Pathology and Genetics Research Unit, USDA-ARS, Davis, CA 95618, USA

Author for correspondence:
Andrew J. McElrone
Tel: +1 530 754 9763
Email: ajmcelrone@ucdavis.edu

Received: *4 October 2017*
Accepted: *23 December 2017*

New Phytologist (2018)
doi: 10.1111/nph.15032

Key words: bark, embolism removal, hydraulic conductivity, *Vitis*, water uptake, woody roots, X-ray computed microtomography (X-ray microCT), xylem.

Summary

- Water acquisition is thought to be limited to the unsuberized surface located close to root tips. However, there are recurring periods when the unsuberized surfaces are limited in woody root systems, and radial water uptake across the bark of woody roots might play an important physiological role in hydraulic functioning.
- Using X-ray microcomputed tomography (microCT) and hydraulic conductivity measurements (Lp_r), we examined water uptake capacity of suberized woody roots *in vivo* and in excised samples.
- Bark hydration in grapevine woody roots occurred quickly upon exposure to water (*c.* 4 h). Lp_r measurements through the bark of woody roots showed that it is permeable to water and becomes more so upon wetting. After bark hydration, microCT analysis showed that absorbed water was utilized to remove embolism locally, where *c.* 20% of root xylem vessels refilled completely within 15 h. Embolism removal did not occur in control roots without water.
- Water uptake through the bark of woody roots probably plays an important role when unsuberized tissue is scarce/absent, and would be particularly relevant following large irrigation events or in late winter when soils are saturated, re-establishing hydraulic functionality before bud break.

Introduction

Woody root systems can be quite extensive (Canadell *et al.*, 1996), spreading in some cases *c.* 50 m laterally and > 50 m in depth (Schenk & Jackson, 2002a,b). The extensive biomass of woody root systems is often classified by size as either suberized woody roots (i.e. with a well-developed bark) or fine roots. In mature forest trees (i.e. yellow poplar), unsuberized fine roots constituted < 1% of the total root surface area, while suberized fine roots constituted up to 50% of total root surface area (Kramer & Bullock, 1966). While unsuberized fine roots are considered to be the primary exchange surface with the soil and responsible for most of the water and nutrient absorption (Kramer & Bullock, 1966; Kramer & Boyer, 1995; Gambetta *et al.*, 2013), there is evidence suggesting that suberized roots could also contribute to water uptake from the soil (Kramer, 1946; MacFall *et al.*, 1990; North & Baker, 2007). To date, it remains largely unknown how much woody roots contribute to plant water absorption under certain scenarios (e.g. when soils are saturated after heavy winter rainfall events or large irrigation events). A more comprehensive understanding of the role of woody roots in overall root-system water uptake could be particularly important for perennial crops like grapevines that have root systems extending to 30 m depth and > 10 m laterally from a vine (Smart *et al.*, 2006), and experience saturated soil conditions periodically after large irrigation events and winter precipitation in many of their growing regions.

The complex branching structure of woody root systems is often classified according to root branch orders that have differential anatomical traits and fulfill distinct functional roles (Guo *et al.*, 2008). Most of the first- and second-order fine roots, which have primary development and dominate the absorptive function, do not persist beyond the current season (Guo *et al.*, 2008). Third-order fine roots transition developmentally into higher orders, where secondary development is clear, and roots display suberized layers and sometimes a well-developed bark (Esau, 1977; Peterson *et al.*, 1993; Peterson & Enstone, 1996; Guo *et al.*, 2008; McCormack *et al.*, 2015). The rate of this transition varies across species, and can be impacted by abiotic and biotic factors. Deposition of suberin and lignin in the apoplast occurs as a normal developmental process in maturing roots, but this process can be hastened by drought stress and is partially responsible for reducing the permeability of these roots (see also Passioura, 1988; North & Nobel, 1991; Nobel & Cui, 1992; North, 2004; Ranathunge *et al.*, 2004; Schreiber *et al.*, 2005; Aroca *et al.*, 2011; Gambetta *et al.*, 2013; Barrios-Masias *et al.*, 2015; Cuneo *et al.*, 2016). During secondary growth, the activity of the vascular and cork cambium produces bark tissue that is composed of inner

bark (i.e. living secondary phloem, phelloderm, dead phloem, and remaining cortex) and outer bark (i.e. old layers of periderm and dead secondary phloem) (Esau, 1977). While the bark tissue helps to protect against insect and pathogen damage (Morris & Jansen, 2016) and prevent water loss in dry soils, less is known about potential water uptake across root bark when the soil is thoroughly wetted or hydraulic properties in other parts of the root system change. Water uptake occurs preferentially in fine root apices, but we recently found that extensive cortical lacunae form in grapevine fine roots under mild drought stress, which dramatically reduced fine root hydraulic conductivity (Lp_r; Cuneo *et al.*, 2016). These types of dynamic changes along with normal development could shift how much water is absorbed by different root portions over time. Interestingly, stem water potentials and stomatal conductance recovered within a day of rewatering for grapevines exhibiting fine root cortical lacunae, even though Lp_r of unsuberized fine roots did not recover (Cuneo *et al.*, 2016). This suggests that water absorption by suberized woody root portions might play a role in drought recovery when unsuberized fine roots become less hydraulically permeable.

Woody roots play a central role in long-distance vascular transport; however, they have been shown to be highly susceptible to xylem embolism formation in several species (Alder *et al.*, 1996; Hacke & Sauter, 1996; McElrone *et al.*, 2004; Pratt *et al.*, 2015; Johnson *et al.*, 2016). Drought stress and winter freezing are two of the main causes of embolism formation (Tyree & Sperry, 1989). Several species have been reported to experience freeze-induced embolism during the winter and subsequent recovery of hydraulic conductivity during the spring via root pressure (Scholander *et al.*, 1955; Sperry *et al.*, 1987, 1988; Wang *et al.*, 1992; Lo Gullo & Salleo, 1993; Cochard *et al.*, 2000; Améglio *et al.*, 2002). In grapevines, xylem embolism in stems can be removed within hours and is associated with the presence of living tissue surrounding vessels (Knipfer *et al.*, 2016). It remains to be shown if the mechanism of embolism removal is the same in woody roots, and if this is possible using water absorbed through the bark of woody roots. A recent study in coastal redwood crowns showed that water uptake through the bark is possible and important for hydraulic recovery (Earles *et al.*, 2015). Similarly, Mayr *et al.* (2014) found that embolism removal in late winter for trees at the alpine timberline was associated with water uptake by needles when frozen soil water was still unavailable.

Here, we aimed to test whether water uptake is possible through the bark of grapevine woody roots, and studied the hydration process of the bark of woody roots using X-ray computed microtomography (microCT). We then used hydraulic measurements to study the radial hydraulic properties of woody roots. While performing the microCT experiments, we discovered that there was a substantial amount of embolism removal in excised stems, and then evaluated these processes in roots *in vivo*. We used florescence microscopy to study the metabolic activity of the xylem tissue in woody roots implicated in this response, and used contact angle measurements of water droplets to study the wettability properties of the bark surface.

Materials and Methods

Plant material

Plants of the grapevine rootstock Millardet et de Grasset 101-14 (101-14 Mgt; *Vitis riparia* × *Vitis rupestris*) were propagated from herbaceous cuttings collected from the experimental vineyards at the University of California, Davis (USA). The propagation consisted of submerging the basal node of a cutting that contained two nodes in 2.5% rooting solution (Earth Science Products, Wilsonville, OR, USA). Subsequently, cuttings were placed in a plastic tray filled with growing medium (50% vermiculite, 50% perlite), and maintained for 15 d in a fog room until there were signs of root initiation (Knipfer *et al.*, 2015). Cuttings were transplanted to 15 l pots filled with soil mix (one-third coarse sand, one-third peat moss and one-third redwood bark compost) and maintained under glasshouse conditions (*c.* 15–25°C temperature, 35% relative humidity, and 16 : 8 h, light : dark cycle) for 8 months. Plants were irrigated once daily with water supplemented with macro- and micronutrients (Gambetta *et al.*, 2013), and shoots were pruned regularly in order to control growth and maintain vigor.

X-ray microCT

X-ray computed microtomography was used to investigate the water-uptake potential through the bark of woody roots. The imaging was performed at beamline 8.3.2 at the Advance Light Source (ALS), Lawrence Berkeley National Laboratory. Plants ($n = 8$) were transported from the University of California, Davis campus, to ALS by car. Once at the ALS, plants were gently removed from the pot, the soil surrounding target roots was removed using a brush (Royal & Langnickel® Essentials™ number 8; Royal & Langnickel, Munster, IN, USA) and suberized woody roots of *c.* 2–3 mm in diameter and *c.* 20 cm long with no laterals were carefully excised using fine-tip scissors. The process of root extraction was performed with special attention, immediately discarding roots with obvious damage. Subsequently, the 20 cm woody root was cut into three segments of *c.* 7 cm that were used for three different treatments (see Fig. 1 for details of sample preparation). Samples from all treatments were scanned over time (> 10 h). In the case of treatments that involved H_2O, water was added into the plastic collar immediately after the first scan. Plants for *in vivo* scanning were prepared by carefully removing the soil of the upper *c.* 10 cm of the pot, exposing woody roots and connecting a plastic collar surrounding the root. Similar to above, water was added to the collar after the first scan; the plastic collar in all experiments was used to control water delivery only to the portion of the root segment being analyzed.

Samples were then fixed to a rotating stage and scanned approximately in the middle of the collar using a 21 keV synchrotron X-ray beam. Samples were scanned multiple times (*c.* 5) in the same position over a period of *c.* 15 h. During scanning, the sample was rotated continuously and 1024 longitudinal images per 180° rotation were collected using a CMOS camera (PCO.edge; PCO AG, Kehlheim, Germany) at a 200 ms

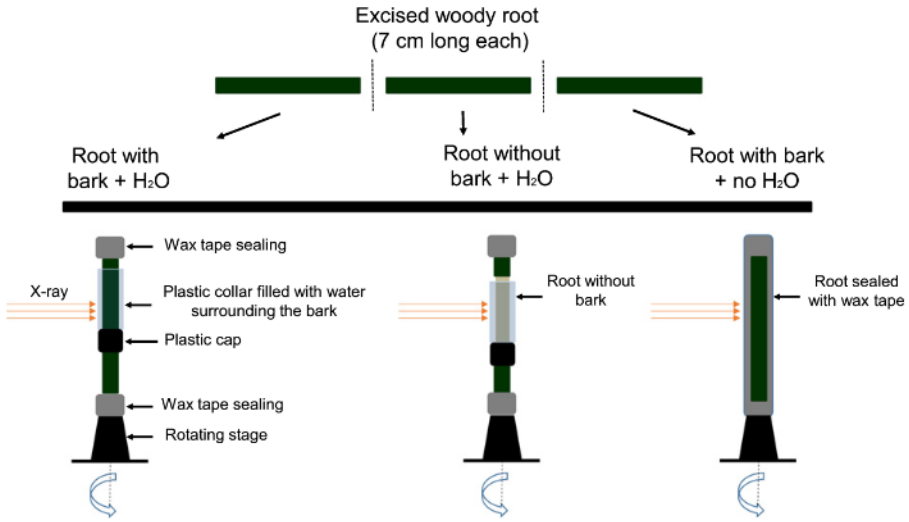

Fig. 1 Illustration of the preparation procedure of excised root samples for X-ray microcomputed tomography imaging. Grapevine woody roots of diameter *c.* 2 mm and length *c.* 20 cm were carefully excised from potted vines. Then, three segments of approximately the same length (*c.* 7 cm) were used for the different treatments. In the root with bark + H_2O treatment, both ends were sealed with wax tape (Parafilm® M; Bemis Co., Oshkosh, WI, USA) to prevent dehydration and a plastic collar filled with water was placed around the bark. For root without bark + H_2O samples, *c.* 3 cm of bark was carefully removed from the excised woody root, sealing both ends with wax tape and placing the plastic collar filled with water around the surface area with no bark. For the root with bark + no H_2O treatment, the whole excised root was sealed using petroleum jelly and wax tape to prevent dehydration. All treatments were scanned over time (> 10 h). In the case of treatments that involved H_2O, water was added to the plastic collar immediately after the first scan.

exposure time. The resolution of images was 4.5 µm pixel^{-1} for *in vivo* scans and 1.3 µm pixel^{-1} for excised roots. The acquired images were reconstructed into a stack of transverse images using OCTOPUS 8.3 software (Institute for Nuclear Sciences, Ghent University, Ghent, Belgium), a custom plugin for FIJI imaging-processing software (www.fiji.sc, IMAGEJ; Schindelin *et al.*, 2012). To analyze the status of water-filled and embolized vessels, reconstructed transverse and longitudinal microCT images were used (Brodersen *et al.*, 2010; Knipfer *et al.*, 2016). The 'slice tool' in AVIZO 9.2.0 software (VSG; FEI Co., Hillsboro, OR, USA) was used to generate longitudinal images from the stack of transverse microCT images. The first scan of each sample was used to determine the number of initially embolized vessels ($N_{\text{initial-embo}}$; Knipfer *et al.*, 2016) and the subsequent scans were used to determine refilled vessels (N_{refilled}), marked in blue using the 'brush' tool, and new embolized vessels (N_{embo}) marked in yellow. The percentage of refilled vessels was calculated as $(N_{\text{refilled}})/(N_{\text{initial-embo}}) \times 100\%$ and the percentage of new embolized vessels was calculated as $(N_{\text{embo}})/(N_{\text{initial-embo}}) \times 100\%$.

For three-dimensional analysis of the porous spaces of the bark, microCT images were masked in FIJI by cropping all parts of the root outside the bark and then thresholding to a consistent pixel value. The grayscale contrast of all three-dimensional images of a given sample was normalized to ensure consistent image segmentation. The stack of images was then loaded into AVIZO 9.2.0 (VSG; FEI Co.), where 'majority' and 'SNN' filters were applied to remove noise, while preserving the features and resolution. After thresholding, the edit label field function was applied to create different materials for the empty pores and the solid bark phases. Finally, the label analysis function was applied to estimate the volume of the different phases (see Supporting Information Fig. S1).

Hydraulic properties of woody roots

After carefully removing the pot, woody roots ($n = 6$) *c.* 2–3 mm in diameter (similar to the ones used in the microCT experiment) were excavated from the soil using a brush (Royal & Langnickel® Essentials™ number 8) and excised using fine-tip scissors. A plastic collar similar to those used in the microCT experiments was then placed around the root (root with bark (not soaked)). One end of the woody root segment was sealed with parafilm (Parafilm®M; Bemis Co.) while the xylem at the other end of the segment was attached to a glass microcapillary (0.25 mm internal diameter; Stoelting Co., Wood Dale, IL, USA) with a stepdown connector. The microcapillary was half-filled with dH_2O and the other end was connected to plastic tubing (1/4 in ID, 1/16 in wall) attached to a vacuum filtration flask (4000 ml; Sigma-Aldrich Inc.) that was attached to a vacuum pump (see Fig. S2 for setup). The flow was measured by tracking the movement of the meniscus in the microcapillary using three pressure steps (i.e. −0.01, −0.02 and −0.03 MPa). Subsequently, the bark was removed from the same root segment and the flow was tracked again (root without bark-not soaked) to quantify how much hydraulic resistance is imposed by the bark. Each hydrostatic pressure step was applied in a downward order (i.e. increasing tension) for 600 s (root with bark-not soaked), and 120 s (root without bark (not soaked)). Volumetric flow rate (Q; m^3 s^{-1}) was obtained for each pressure step using the equation, volumetric flow rate $= (\pi(r^2)d) \times 1/t$, where r is the radius of the microcapillary, d is the distance traveled by the meniscus, and t is time (in s). The hydraulic conductance (C; m^3 s^{-1} MPa^{-1}) was calculated as the slope of the linear regression line between Q and the hydrostatic pressure gradient (ΔP; see Fig. S3). The surface area (A; m^2) of the root segment was measured using WINRHIZO (WinRhizo

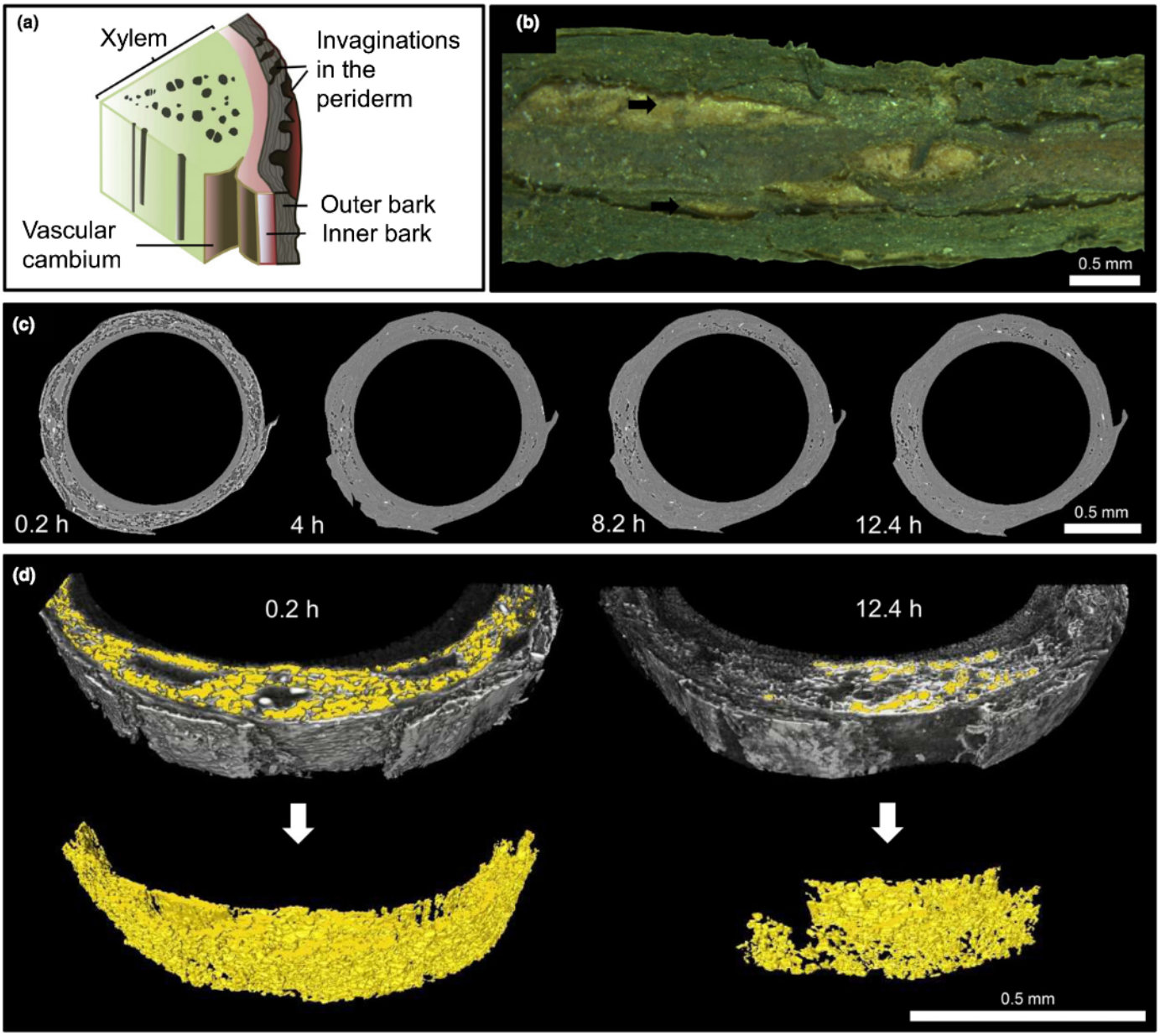

Fig. 2 (a) Illustration showing the anatomy of the grapevine woody roots that were analyzed. The bark corresponds to the tissue outside the vascular cambium composed of inner (i.e. living secondary phloem, phelloderm, dead phloem, and remaining cortex) and outer bark (i.e. old layers of periderm, dead secondary phloem, outside of cork cambium). (b) Representative top view of a woody root showing the bark surface with ruptured layers of periderm (indicated by black arrows). (c) Representative time series of transverse X-ray microcomputed tomography images through woody roots showing the bark. After the first image ($t = 0.2$ h), the surface of the root was exposed to water and continued to be imaged in the same place. The air (dark gray) in the bark tissue was replaced by water (light gray, i.e. bark hydration) over time. (d) Representative three-dimensional volume rendering of a portion of the bark in (c) ($t = 0.2$ and 12.4), visualizing the decline in air-filled volume (indicated in yellow) during bark hydration.

Pro 2009b; Régent Instruments Inc., Ville de Québec, QC, Canada) and the hydraulic conductivity (Lp_r; m s^{-1} MPa^{-1}) was calculated as $Lp_r = C/A$. Lp_r was also obtained on roots with intact bark that were soaked in water for 24 h before measurement (root with bark-soaked) using the same procedure described earlier.

Fluorescein-diacetate-propidium iodide staining

Cell viability was assessed with fluorescent light microscopy in root segments that were stained simultaneously with a 9.6 µM fluorescein-diacetate (FDA; Sigma-Aldrich Inc.) and a 2.9 µM propidium iodide solutions (PI; Sigma-Aldrich Inc.). The FDA-PI staining solution was prepared by adding 8 µl FDA and 50 µl PI to 5 ml of water. Plants ($n = 5$) were transported from the glasshouse to the laboratory and the woody roots (with the same characteristics as in previous experiments) were collected. Transverse segments were cut using a fresh razor blade and were immediately submerged in the staining solution for 30 min and incubated in the dark at *c.* 23°C. A second set of roots was placed in a −70°C freezer for 3 d after excision to decrease any

metabolic activity. After 3 d, transverse segments were cut and stained as described previously. Samples were mounted on glass slides and observed under fluorescent light (excitation filter 490 and 575 nm, dichromatic mirror 505 nm, barrier filter 525 and 625 nm) for detection of living and dead tissue. The microscope used was a Leica DM4000 B LED equipped with a Leica DFC7000 T 2.8 MP camera (Buffalo Grove, IL, USA).

Wettability of the bark

Wettability properties of the bark of woody roots were studied using a custom-made contact angle meter that consisted of a stereoscope (Fisher Scientific, Waltham, MA, USA) inverted to 90° and equipped with a Leica DFC 295 camera. A 1 µl sessile drop of distilled water was generated using a 3D printed syringe pump (Wijnen *et al.*, 2014) connected to a Stoelting mechanical micromanipulator (Stoelting Co.). Excised roots were placed in a glass stage with the open end facing the objective lens of the stereoscope. The advancing contact angle (θ) was measured at room temperature (25°C) by capturing side view images of the drops at a rate of 3 frames s^{-1}. Contact angles, surface area of contact (mm^2) and drop volume (µl) were calculated automatically from the photographic images using a low-bond axisymmetric drop shape analysis method based on the Young–Laplace equation (see Stalder *et al.*, 2010). This analysis method has been implemented as a Java plugin for the ImageJ software (www.fiji.sc, ImageJ; Schindelin *et al.*, 2012).

Statistical analysis

Analysis of variance (ANOVA) was performed using R v.3.3.2 statistical computing environment (R Core Team, 2016) with the aid of the car software package (Fox & Weisberg, 2011). The Shapiro–Wilk and Levene tests were used to check for normality and homogeneity of variance, respectively. Data were transformed as necessary when assumptions were not met. Tukey' honest significant difference test was used to determine significant differences among treatments.

Results

All roots examined had a well-developed bark layer containing a rough surface with obvious invaginations in the periderm (Fig. 2a,b), but also an inner bark composed of living secondary phloem, phelloderm, dead phloem, and remaining cortex (Fig. 2a). Bark hydration was obvious after *c.* 4 h and continued overtime as the small air-filled spaces of the bark filled with water (Fig. 2c,d). Using porosity analysis to estimate temporal changes of the volume of empty pores in each image stack, we found that *c.* 32% of the bark volume was composed of empty pores before exposure to water (i.e. $t = 0$; Fig. 3). The air-filled volume fraction dropped precipitously to *c.* 4.6% after *c.* 4 h (reduction of *c.* 85% of empty pores in the first *c.* 4 h; Fig. 3).

In the root with bark + H_2O treatment, embolism removal started *c.* 2 h after the bark was exposed to water (Fig. 4a; indicated in blue color). After *c.* 15 h, 20.2% of the originally

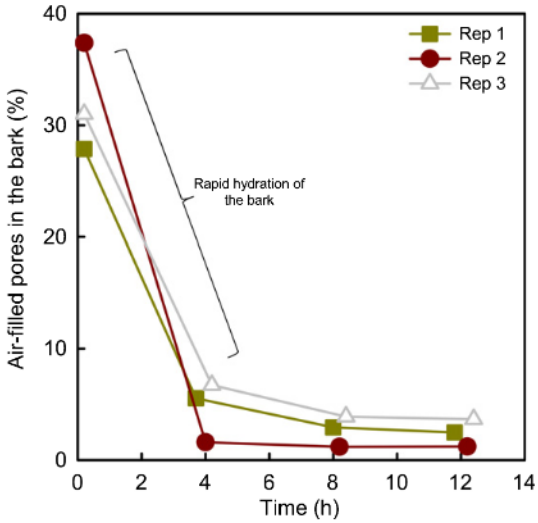

Fig. 3 Temporal changes in the percentage of air-filled pores in the bark of grapevine woody roots as a consequence of bark hydration. Data were obtained from X-ray microcomputed tomography image stacks (see Fig. 1c and Supporting Information Fig. S1 as example), using a three-dimensional porosity analysis procedure.

embolized vessels had refilled (Fig. 4a). Embolism formation after bark rehydration started was rarely observed in the root with bark + H_2O treatment (Fig. 4a, indicated in yellow). When the bark was removed from the roots and water was provided surrounding the surface of the root (i.e. root without bark + H_2O), the percentage of refilled vessels increased rapidly over time (Fig. 4b). The estimated time required to fill 100% of the embolized vessels was 18 h, and around five times faster than in the root with bark + H_2O treatment (Fig. 5b). Also, a linear regression was performed for every repetition (Fig. 5), and we found that the mean slope for the root with bark + H_2O treatment (1.11 ± 0.26 SE) was significantly lower than that of the root without bark + H_2O treatment (7.25 ± 1.28; $P = 0.002$). In the case of the root with bark + no H_2O treatment, the root segment was completely sealed, and we observed a mean increase of 41.1% in embolism formation after *c.* 14.8 h and little embolism removal (Fig. 4c).

To verify that patterns in excised roots were consistent with attached-intact roots, bark hydration and embolism removal were also observed *in vivo* (Fig. 6). Both processes of bark hydration and embolism removal were apparent in attached-intact roots within 12 h after the surface of the root was exposed to water (Fig. 6). Both bark hydration and embolism removal via droplet growth and water column expansion were qualitatively similar between *in vivo* scanning and excised roots (Figs 6, S4).

We measured the radial hydraulic properties of woody roots using a vacuum-based hydrostatically driven water flow. The volumetric flow rate responded linearly to the increase of vacuum-based pressure steps used in this experiment (i.e. −0.01, −0.02, −0.03 MPa; Fig. S3). The roots with bark (not soaked) treatment showed a mean (± SE) Lp_r value of 4.3E–8 ± 9.8E–9 m s^{-1} MPa^{-1}, while the Lp_r of the roots with bark (soaked) treatment was around eight times greater (3.5E–7 ± 1.6E–7 m s^{-1} MPa^{-1}; see Fig. 7). The Lp_r of the roots without bark (not

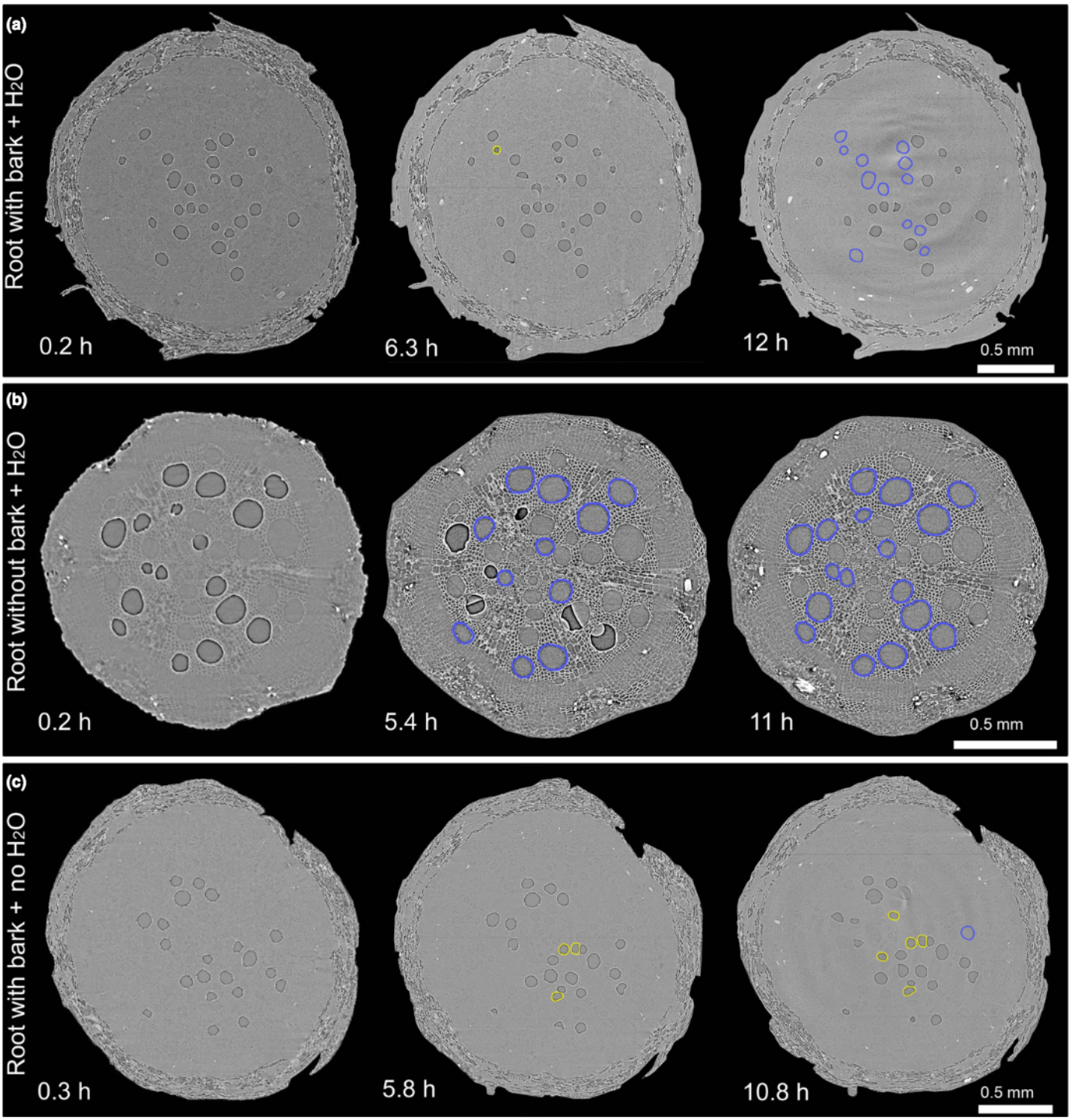

Fig. 4 Representative time series of transverse X-ray microcomputed tomography images through excised woody roots of grapevine. (a) Root with bark and supplied with H_2O (root with bark + H_2O). (b) Root without bark and supplied with H_2O (root without bark + H_2O). (c) Root completely sealed with wax tape and no water supplied (root with bark + no H_2O). Water-filled tissue appears light gray while air-filled tissue appears dark gray. After excision, refilled vessels are highlighted in blue, while new embolized vessels are highlighted in yellow.

soaked) treatment was *c.* 20 times larger than that observed for roots with bark (8.6E–7 ± 1.5E–7 $m\,s^{-1}\,MPa^{-1}$; Fig. 7; mean values were significantly different at $P < 0.005$).

An FDA-PI dual staining technique was used to visualize metabolically active and inactive cells of the woody root tissue simultaneously. Transverse woody root sections stained with FDA-PI showed metabolic activity (i.e. green fluorescence signal) in the xylem tissue surrounding the vessels (Fig. 8a,b). This method showed that a large proportion of the xylem tissue in woody roots is composed of living cells at maturity, including the

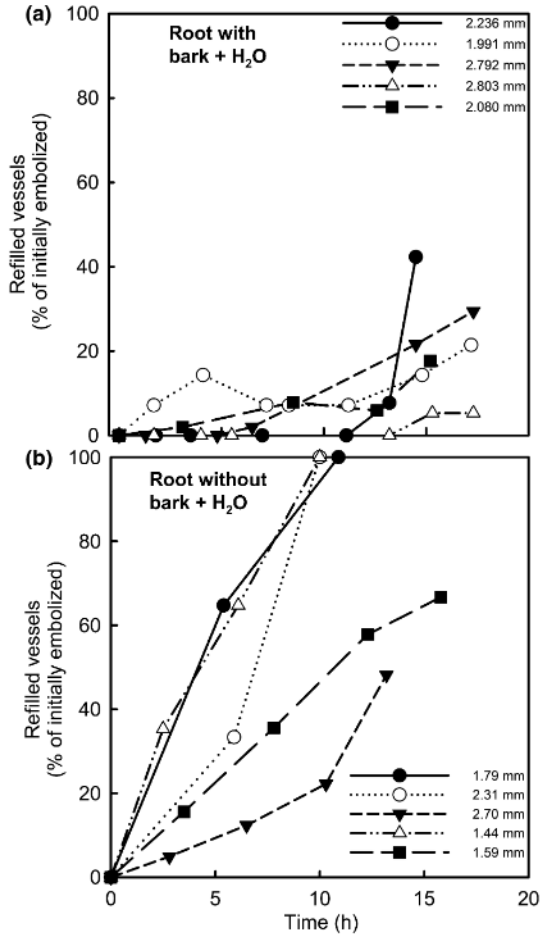

Fig. 5 Temporal changes of refilled vessels (presented as % of initially embolized) in excised woody roots obtained from grapevine plants. (a, b) Following excision ($t = 0$ h), woody roots were supplied with H_2O (root with bark + H_2O) (a) and bark was removed after excision ($t = 0$ h) and H_2O was supplied (root without bark + H_2O) (b). Values in legends are diameters of roots used.

fibers. The green fluorescence signal was strongest in the axial and ray parenchyma. The PI dye (red fluorescence signal) remained in intercellular spaces and the walls of vessels (Fig. 8b), and there was no sign of stained nuclei of cells, indicating that cells of the xylem tissue of woody roots were metabolically active with an intact cell membrane (Fig. 8b).

To understand the wettability properties of the bark of woody roots, we observed the behavior of water droplets that were deposited on the surface of the bark. A steady contact angle value was found immediately after depositing the drop in the bark surface. The mean advancing contact angle of drops of water on the surface of the bark was $100.6 \pm 4.2°$. We found a negative relationship between the surface area of contact at the droplet–bark interface and the contact angle (Fig. S5).

Discussion

The results presented here provide direct evidence that water uptake can occur radially across woody roots of grapevines. Not only did we observe that water can enter woody roots through the lignified and suberized bark layer, pointing to the water uptake potential of these roots, but unexpectedly bark hydration and uptake across this surface were linked with the formation of droplets on xylem vessel walls that are associated with embolism repair processes. We observed similar patterns in both excised samples and *in vivo* that were similar to the mechanism we described previously for grapevine stems (Brodersen *et al.*, 2010; Knipfer *et al.*, 2015, 2016). Hydraulic conductivity measurements revealed that woody roots are permeable to water, and this permeability tends to increase after bark hydration (i.e. roots with bark, soaked). Even though the Lp_r of unsuberized fine roots is considerably higher, the results presented here could be particularly applicable during periods when fine roots are scarce or damaged, or have lost contact with the surrounding soil (e.g. during or after a drought). Several studies have also shown that root pressure plays an important role in repairing xylem conduits that embolized from winter freeze–thaw events (Scholander *et al.*, 1955; Sperry *et al.*, 1987, 1988; Lo Gullo & Salleo, 1993; Cochard *et al.*, 2000; Améglio *et al.*, 2002). Limited fine roots during winter and early spring when freeze–thaw events are prevalent might allow for absorption through the woody tissue as seen here, thereby activating the root system and restoring hydraulic capacity before spring xylogenesis and fine root development.

Woody root systems are classified based on the branching order system where different branch orders have different anatomical and functional characteristics (Guo *et al.*, 2008; McCormack *et al.*, 2015). First- and second-order roots are commonly unsuberized or less suberized and have greater hydraulic permeability compared with higher-order roots (Guo *et al.*, 2008; McCormack *et al.*, 2015). The literature indicates that the bulk of water absorption occurs in unsuberized fine roots (e.g. Taiz & Zeiger, 2015), but water uptake through woody root portions (i.e. typically fourth- or higher-order roots) might be of significance when the absorption pathways of fine roots are scarce or damaged (Green & Clothier, 1999; Dubrovsky & North, 2002; Cuneo *et al.*, 2016). Direct evidence using hydraulic measurements from Queen (1967) and Chung & Kramer (1975) found that significant amounts of water and phosphorus uptake can occur through woody roots, and MacFall *et al.* (1990) used magnetic resonance imaging (MRI) to detect soil water depletion surrounding suberized tap roots of pine. For this latter study, it is not known whether water was absorbed somewhere else along the root length and just pulled as a film from the point imaged with MRI. Previous studies suggest that hydraulically isolated soil compartments are needed to rule this out completely (Zarebanadkouki *et al.*, 2013; Zarebanadkouki & Carminatti, 2014), and the methods used here provided water only to the woody portion of the root that was scanned.

The present data show that for water absorption to occur, water needs to be freely available for several hours before hydration of the bark is clearly visible (see Figs 2c, 3–5), which can commonly occur after heavy or prolonged rainfall events or large irrigation events. It is important to highlight that the process of bark hydration occurred quite quickly (*c.* 4 h), with the water moving initially through small pores in the bark (see Fig. 2) and then probably through both symplastic and apoplastic pathways.

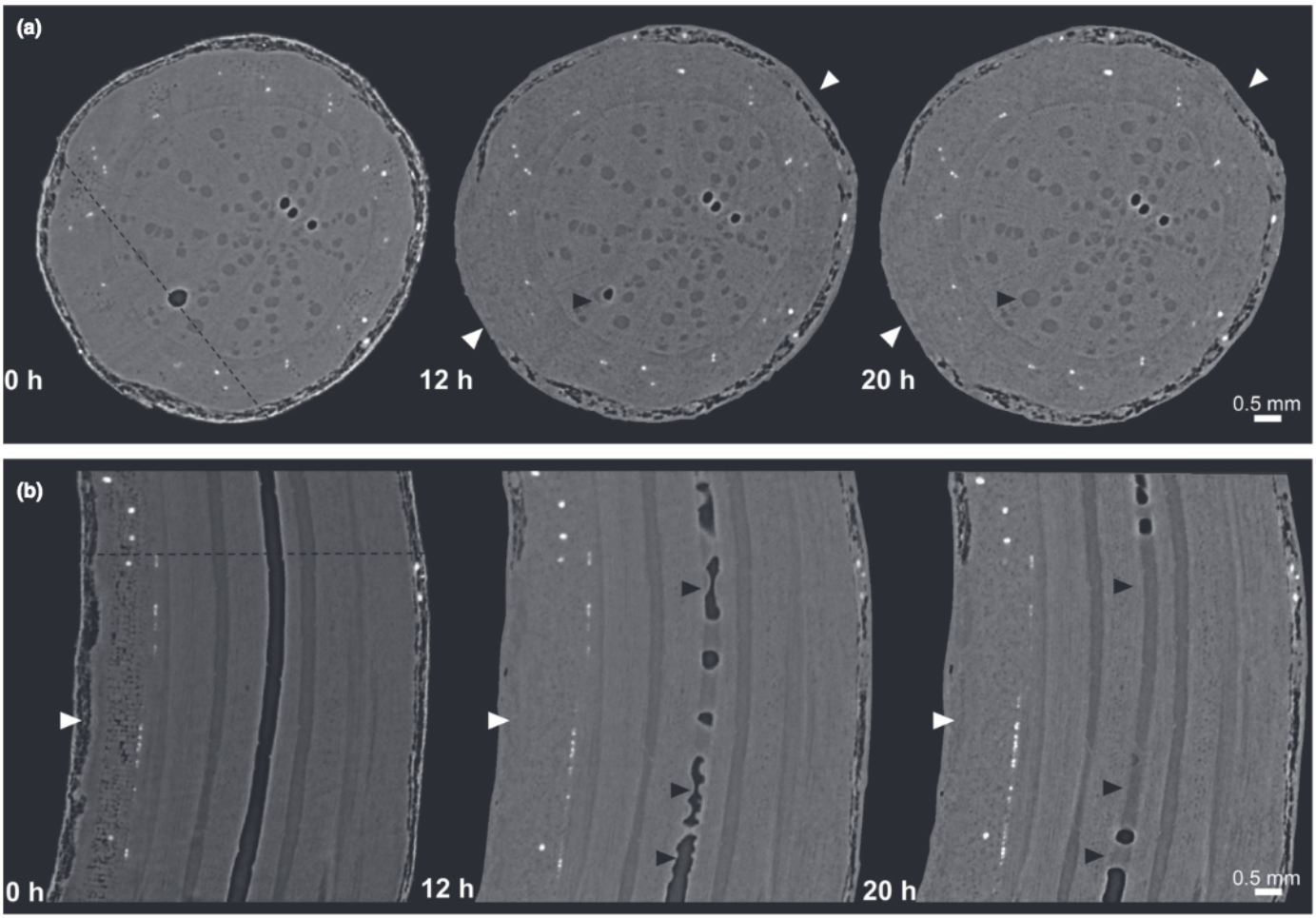

Fig. 6 Bark hydration and process of vessel refilling observed *in vivo* in grapevine woody roots using X-ray microcomputed tomography (microCT) and scanning in the same position at different times. Hydration of the bark is obvious and indicated with white arrowheads in (a) and (b). In (b), longitudinal microCT images show the process of embolism removal via the process of water droplet growth and water column expansion (indicated with black arrowheads).

A similar phenomenon was recently documented in two studies of plant canopies. Water was absorbed through woody stems of coastal redwood, leading to hydraulic recovery (Earles *et al.*, 2015), which could be particularly important in foggy habitats and for a species with tremendous above-ground woody surface area. Mayr *et al.* (2014) also observed that embolism refilling occurred from snowmelt during the late winter in trees at the alpine timberline when water was not yet available from still-frozen soil. Radial water uptake in woody roots is even more likely given the saturated conditions that can often occur in soils, but more research is needed to better understand the properties of bark of different species under varied growing conditions.

Drought and/or freezing stress can cause xylem embolism that minimizes water transport capacity and can lead to plant mortality (Tyree & Sperry, 1989). In grapevine, xylem vessels have been reported to be gas-filled during the winter and recover their hydraulic capacity via root pressure in the spring (Scholander *et al.*, 1955; Sperry *et al.*, 1987). This spring xylem refilling is considered critical in many species by enabling root systems to conduct water to activate dormant buds and initiate leaf expansion, which occurs before new xylem vessels have differentiated

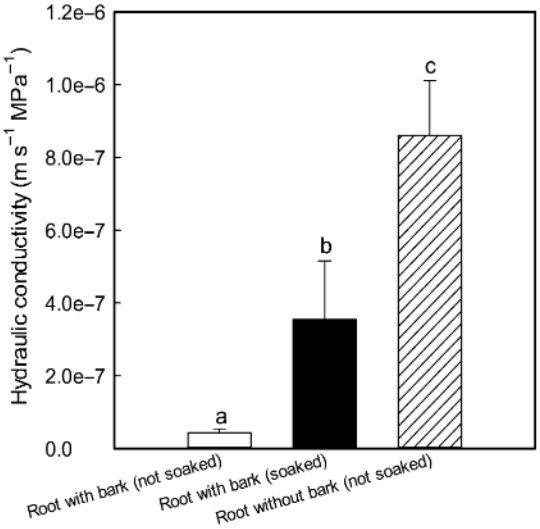

Fig. 7 Radial root hydraulic conductivity (Lp_r) of grapevine roots with bark (not soaked), roots with bark (soaked) (i.e. root with bark soaked in water for 24 h) and roots without bark (not soaked). Data are means ± SE ($n = 6$). Means followed by different letters are significantly different at $P < 0.05$.

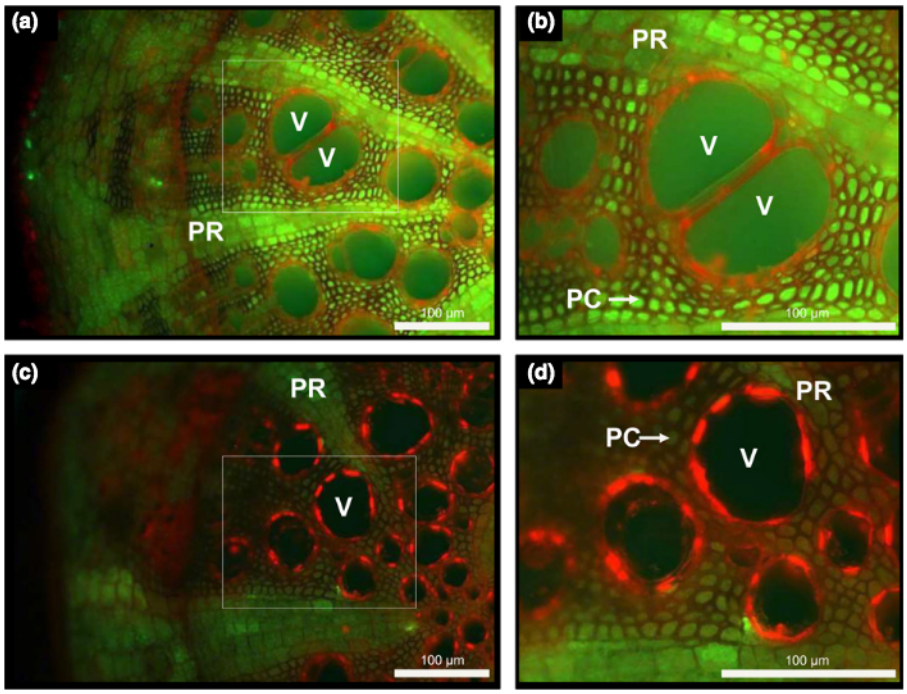

Fig. 8 Transverse woody root sections of grapevine stained with fluorescein-diacetate/propidium-iodide and observed under fluorescent light (G/R filter system for blue and green excitation). The lumen of metabolically active cells appears in green (fluorescein signal), while cell walls (apoplast) and nucleus of nonviable cells are stained in red. (a, b) Cross-section images of roots collected and stained immediately after excision. The intensity of the fluorescein signal is stronger in cells that compose the parenchyma rays compared with tissue surrounding vessels (a). (c, d) Cross-section images of roots that were first exposed to −70°C for 3 d and stained after the treatment. Green fluorescence signal was substantially reduced. V, vessel; PR, parenchyma ray; PC, parenchyma cell.

(Sperry *et al.*, 1987; Cochard *et al.*, 2000). Recently, Knipfer *et al.* (2016) demonstrated that xylem refilling in excised grapevine stems can occur in the absence of root pressure and is locally driven by vessel-associated tissue. Our current data provide *in vivo* evidence that the embolism removal process is similar in grapevine roots. The mechanism seen here of water droplet growth from the lateral walls of embolized vessels appears qualitatively similar to that observed in grapevine stems (Brodersen *et al.*, 2010, 2013; Knipfer *et al.*, 2015, 2016). Moreover, xylem tissue in woody roots was composed of vast amounts of metabolically active cells surrounding vessels, suggesting that droplet growth and embolism removal in these roots is driven by vessel-associated tissue, as suggested previously (Brodersen *et al.*, 2010; Knipfer *et al.*, 2016; Secchi & Zwieniecki, 2016).

In excised grapevine stems, the time needed to fill 100% of the embolized vessels was *c.* 5 h (Knipfer *et al.*, 2016). In contrast, the calculated average time required to fill 100% of the embolized vessels in woody roots is several times higher (i.e. extrapolation to 96.5 h in the root with bark + H_2O treatment assuming that the refilling rate is constant over time). We speculate that this difference in temporal dynamics of embolism removal between roots and stems arises because, in the case of woody roots, water needed first to traverse the outer and inner bark layers before arriving in the xylem (see Fig. 1a). Interestingly, the hydraulic resistance of the bark decreases when it has been soaked, and the refilling rate increases 5.3 times when the bark is removed, illustrating the high hydraulic resistivity of the bark. Similar hydraulic properties were previously reported by Queen (1967) on excised segments only. The wettability properties of the bark shown here (i.e. *c.* 100° advancing contact angle) illustrate the hydrophobicity of the bark material of these roots which could certainly contribute to the hydraulic resistivity of the material. Nevertheless, embolism removal by water supplied radially across the woody roots could be very important for rapid recovery of hydraulic conductivity under saturated soil conditions. Understanding the complex water relations dynamics of woody root systems, with roots spreading several meters laterally and to greater depths, and the ecological impact of the distribution and function of these roots are important studies for the future.

The radial hydraulic properties of woody roots remain largely unknown, whereas hydraulics of nonwoody roots have been studied extensively (e.g. Steudle & Peterson, 1998; Knipfer & Fricke, 2011; Gambetta *et al.*, 2012, 2013; Barrios-Masias *et al.*, 2015; Cuneo *et al.*, 2016). In general, it is known that the hydraulic resistance per unit root length decreases toward the tip (Meyer & Ritchie, 1980), but it has been modeled that half of the water absorbed in Barley roots occurs in older suberized regions (Sanderson, 1983). There are a few studies that effectively reported the radial hydraulic conductivity of woody roots (exceptions are Kramer, 1946; Queen, 1967; North & Nobel, 1991). Queen (1967) observed that the relative permeability of grapevine woody roots (i.e. heavily suberized, thick bark) was one-fifth of the relative permeability of nonsuberized roots (i.e. terminal 8 cm, elongating, unbranched, unsuberized). Our results reflect the enormous resistance imposed by bark, but the bark is

permeable and its properties can change with wetting to facilitate water uptake under saturated conditions. The data presented here suggest that under conditions in which fine roots are actively growing, water uptake will occur preferentially through those regions because they confer less resistance to water flow (see Zwieniecki *et al.*, 2002). However, under conditions in which fine roots are damaged (i.e. after a drought; Cuneo *et al.*, 2016) or simply scarce/absent (i.e. winter), shifts in water uptake to woody root portions might explain the recovery of water potentials after rewatering or activation or root systems in the spring.

Acknowledgements

I.F.C. received funding through the Katherine Esau Graduate fellowship program. This work was supported by funding from the American Vineyard Foundation to A.J.M. and USDA-ARS CRIS funding (grant no. 5306-21220-004-00). The Advanced Light Source is supported by the Director, Office of Science, Office of Basic Energy Science, of the US Department of Energy under contract no. DE-AC02-05CH11231.The authors kindly thank D. Parkinson and A. MacDowell for their assistance at the Lawrence Berkeley National Laboratory Advanced Light Source (ALS) Beamline 8.3.2 microtomography facility. The authors kindly thank Andy Walker and Astrid Volder for critically reading and revising the article. Thanks also to J. Uretsky for help with plant preparation and Clarissa Reyes for help with image analysis.

Author contributions

I.F.C. and A.J.M. designed the experiments. I.F.C. and T.K. performed the microCT scanning; I.F.C. and P.M. performed the image analysis. I.F.C. performed root hydraulics and microscopy essays; I.F.C. and A.J.M. wrote the initial draft of the article; T.K., P.M. and C.R.B. revised and edited the article; C.R.B. and A.J.M. obtained funding and microCT beam time; A.J.M. supervised the project.

References

Alder NN, Sperry JS, Pockman WT. 1996. Root and stem xylem embolism, stomatal conductance, and leaf turgor in *Acer grandidentatum* populations along a soil moisture gradient. *Oecologia* **105**: 293–301.

Améglio T, Bodet C, Lacointe A, Cochard H. 2002. Winter embolism, mechanisms of xylem hydraulic conductivity recovery and springtime growth patterns in walnut and peach trees. *Tree Physiology* **22**: 1211–1220.

Aroca R, Porcel R, Ruiz-Lozano JM. 2011. Regulation of root water uptake under abiotic stress conditions. *Journal of Experimental Botany* **63**: 43–57.

Barrios-Masias FH, Knipfer TM, McElrone AJ. 2015. Differential responses of grapevine rootstocks to water stress are associated with adjustments in fine root hydraulic physiology and suberization. *Journal of Experimental Botany* **66**: 6069–6078.

Brodersen CR, McElrone AJ, Choat B, Lee E, Shackel KA, Matthews MA. 2013. *In vivo* visualizations of drought-induced embolism spread in *Vitis vinifera*. *Plant Physiology* **161**: 1820–1829.

Brodersen CR, McElrone AJ, Choat B, Matthews MA, Shackel KA. 2010. The dynamics of embolism repair in xylem: *in vivo* visualizations using high-resolution computed tomography. *Plant Physiology* **154**: 1088–1095.

Canadell J, Jackson RB, Ehleringer JR, Mooney HA, Sala OE, Schulze ED. 1996. Maximum rooting depth of vegetation types at the global scale. *Oecologia* **108**: 583–595.

Chung HH, Kramer PJ. 1975. Absorption of water and ^{32}P through suberized and unsuberized roots of loblolly pine. *Canadian Journal of Forest Research* **5**: 229–235.

Cochard H, Lemoine D, Améglio T, Granier A. 2000. Mechanisms of xylem recovery from winter embolism in *Fagus sylvatica*. *Tree Physiology* **21**: 27–33.

Cuneo IF, Knipfer T, Brodersen CR, McElrone AJ. 2016. Mechanical failure of fine root cortical cells initiates plant hydraulic decline during drought. *Plant Physiology* **172**: 1669–1678.

Dubrovsky JG, North GB. 2002. Root structure and function. In: Nobel PS, ed. *Cacti: biology and uses*. Berkeley, CA, USA: University of California Press, Berkeley, 41–56.

Earles JM, Sperling O, Silva LCR, McElrone AJ, Brodersen CR, North MP, Zwieniecki MA. 2015. Bark water uptake promotes localized hydraulic recovery in coastal redwood crown. *Plant Cell and Environment* **39**: 320–328.

Esau K. 1977. *Anatomy of seed plants, 2nd edn.* New York, NY, USA: Wiley.

Fox J, Weisberg S. 2011. *An R companion to applied regression, 2nd edn.* Thousand Oaks CA: Sage. [WWW document] URL http://socserv.socsci.mcmaster.ca/jfox/Books/Companion [accessed 2 July 2018].

Gambetta GA, Fei J, Rost TL, Knipfer T, Matthews MA, Shackel KA, Walker MA, McElrone AJ. 2013. Water uptake along the length of grapevine fine roots: developmental anatomy, tissue-specific aquaporin expression, and pathways of water transport. *Plant Physiology* **163**: 1254–1265.

Gambetta GA, Manuck CM, Drucker ST, Shaghasi T, Fort K, Matthews MA, Walker MA, McElrone AJ. 2012. The relationship between root hydraulics and scion vigour across *Vitis* rootstocks: what role do root aquaporins play? *Journal of Experimental Botany* **63**: 6445–6455.

Green S, Clothier B. 1999. The root zone dynamics of water uptake by a mature apple tree. *Plant and Soil* **206**: 61–77.

Guo D, Xia M, Wei X, Chang W, Liu Y, Wang Z. 2008. Anatomical traits associated with absorption and mycorrhizal colonization are linked to root branch order in twenty-three Chinese temperate tree species. *New Phytologist* **180**: 673–683.

Hacke U, Sauter JJ. 1996. Drought-induced xylem dysfunction in petioles, branches, and roots of *Populus balsamifera* L. and *Alnus glutinosa* (L.) Gaertn. *Plant Physiology* **111**: 413–417.

Johnson DM, Wortemann R, McCulloh KA, Jordan-Meille L, Ward E, Warren JM, Palmroth S, Domec JC. 2016. A test of the hydraulic vulnerability segmentation hypothesis in angiosperm and conifer tree species. *Tree Physiology* **36**: 983–993.

Knipfer T, Cuneo IF, Brodersen CR, McElrone AJ. 2016. *In-situ* visualization of the dynamics in xylem embolism formation and removal in the absence of root pressure: a study on excised grapevine stems. *Plant Physiology* **171**: 1024–1036.

Knipfer T, Eustis AJ, Brodersen CR, Walker MA, McElrone AJ. 2015. Grapevine species from varied native habitats exhibit differences in embolism formation/repair associated with leaf gas exchange and root pressure. *Plant, Cell & Environment* **38**: 1503–1513.

Knipfer T, Fricke W. 2011. Water uptake by seminal and adventitious roots in relation to whole-plant water flow in barley (*Hordeum vulgare* L.). *Journal of Experimental Botany* **62**: 717–733.

Kramer PJ. 1946. Absorption of water through suberized roots of trees. *Plant Physiology* **21**: 37–41.

Kramer PJ, Boyer JS. 1995. *Water relations of plant and soil.* San Diego, CA, USA: Academic Press.

Kramer PJ, Bullock HC. 1966. Seasonal variation in the proportions of suberized and unsuberized roots of trees in relation to the absorbed water. *American Journal of Botany* **53**: 200–204.

Lo Gullo MA, Salleo S. 1993. Different vulnerabilities of *Quercus ilex* L. to freeze- and summer drought-induced xylem embolism: an ecological interpretation. *Plant, Cell & Environment* **16**: 511–519.

MacFall JS, Johnson GA, Kramer PJ. 1990. Observation of a water depletion region surrounding loblolly pine roots by magnetic resonance imaging. *Proceedings of the National Academy of Sciences, USA* **87**: 1203–1207.

Mayr S, Schmid P, Laur J, Rosner S, Charra-Vaskou K, Dämon B, Hacke UG. 2014. Uptake of water via branches helps timberline conifers refill embolized xylem in late winter. *Plant Physiology* **164**: 1731–1740.

McCormack ML, Dickie IA, Eissenstat DM, Fahey TJ, Fernandez CW, Guo D, Helmisaari HS, Hobbie EA, Iversen CM, Jackson RB *et al.* 2015. Redefining fine roots improves understanding of below-ground contributions to terrestrial biosphere processes. *New Phytologist* **207**: 505–518.

McElrone AJ, Pockman WT, Martínez-Vilalta J, Jackson RB. 2004. Variation in xylem structure and function in stems and roots of trees to 20 m depth. *New Phytologist* **163**: 507–517.

Meyer WS, Ritchie JT. 1980. Water status of cotton as related to taproot length. *Agronomy Journal* **70**: 981–986.

Morris M, Jansen S. 2016. Bark: its anatomy, function and diversity. *International dendrology society yearbook.* Kington, UK: International Dendrology Society, 51–61.

Nobel PS, Cui M. 1992. Hydraulic conductances of the soil, the root-soil air gap, and the root: changes for desert succulents in drying soil. *Journal of Experimental Botany* **43**: 319–326.

North G. 2004. A long drink of water: how xylem changes with depth. *New Phytologist* **163**: 447–449.

North GB, Baker EA. 2007. Water uptake by older roots: evidence from desert succulents. *HortScience* **42**: 1103–1106.

North GB, Nobel PS. 1991. Changes in hydraulic conductivity and anatomy caused by drying and rewetting roots of *Agave deserti* (Agavaceae). *American Journal of Botany* **78**: 906–915.

Passioura JB. 1988. Water transport in and to roots. *Annual Review of Plant Physiology and Plant Molecular Biology* **39**: 245–265.

Peterson CA, Enstone DE. 1996. Functions of passage cells in the endodermis and exodermis of roots. *Physiologia Plantarum* **97**: 592–598.

Peterson CA, Murrmann M, Steudle E. 1993. Location of the major barriers to water and ion movement in young roots of *Zea mays* L. *Planta* **190**: 127–136.

Pratt RB, MacKinnon ED, Venturas MD, Crous CJ, Jacobsen AL. 2015. Root resistance to cavitation is accurately measured using a centrifuge technique. *Tree Physiology* **35**: 185–196.

Queen WH. 1967. *Radial movement of water and ^{32}P through suberized and unsuberized roots of grape.* PhD thesis. Duke University, Durham, NC, USA.

R Core Team. 2016. *R: A language and environment for statistical computing.* Vienna, Austria: R Foundation for Statistical Computing. [WWW document] URL http://www.R-project.org/ [accessed 2 July 2018].

Ranathunge K, Kotula L, Steudle E, Lafitte R. 2004. Water permeability and reflection coefficient of the outer part of young rice roots are differently affected by closure of water channels (aquaporins) or blockage of apoplastic pores. *Journal of Experimental Botany* **55**: 433–447.

Sanderson J. 1983. Water uptake by different regions of the barley root: pathways of radial flow in relation to development of the endodermis. *Journal of Experimental Botany* **34**: 240–253.

Schenk HJ, Jackson RB. 2002a. Rooting depths, lateral root spreads and below-ground/above-ground allometries of plants in water-limited ecosystems. *Journal of Ecology* **90**: 480–494.

Schenk HJ, Jackson RB. 2002b. The global biogeography of roots. *Ecological Monographs* **72**: 311–328.

Schindelin J, Arganda-Carreras I, Frise E, Kaynig V, Longair M, Pietzsch T, Preibisch S, Rueden C, Saalfeld S, Schmid B *et al.* 2012. Fiji: an open-source platform for biological-image analysis. *Nature Methods* **9**: 676–682.

Scholander PF, Love WE, Kanwisher JW. 1955. The rise of sap in tall grapevines. *Plant Physiology* **30**: 93–104.

Schreiber L, Franke R, Hartmann K, Ranathunge K, Steudle E. 2005. The chemical composition of suberin in apoplastic barriers affects radial hydraulic conductivity differently in the roots of rice (*Oryza sativa* L. cv. IR64) and corn (*Zea mays* L. cv. Helix). *Journal of Experimental Botany* **56**: 1427–1436.

Secchi F, Zwieniecki MA. 2016. Accumulation of sugars in the xylem apoplast observed under water stress conditions is controlled by xylem pH. *Plant, Cell & Environment* **39**: 2350–2360.

Smart DR, Schwass E, Lakso A, Morano L. 2006. Grapevine rooting patterns: a comprehensive analysis and review. *American Journal of Enology and Viticulture* **57**: 89–104.

Sperry JS, Donnelly JR, Tyree MT. 1988. Seasonal occurrence of xylem embolism in sugar maple (*Acer saccharum*). *American Journal of Botany* **75**: 1212–1218.

Sperry JS, Holbrook NM, Zimmermann MH, Tyree MT. 1987. Spring filling of xylem vessels in wild grapevine. *Plant Physiology* **83**: 414–417.

Stalder AF, Melchior T, Müller M, Sage D, Blu T, Unser M. 2010. Low-bond axisymmetric drop shape analysis for surface tension and contact angle measurements of sessile drops. *Colloids and Surfaces A: Physicochemical and Engineering Aspects* **364**: 72–81.

Steudle E, Peterson CA. 1998. How does water get through roots? *Journal of Experimental Botany* **49**: 775–788.

Taiz L, Zeiger E. 2015. *Plant physiology and development.* Sunderland, MA, USA: Sinauer Associates.

Tyree MT, Sperry JS. 1989. Vulnerability of xylem to cavitation and embolism. *Annual Review of Plant Physiology and Plant Molecular Biology* **40**: 19–38.

Wang J, Ives NE, Lechowicz MJ. 1992. The relation of foliar phenology to xylem embolism in trees. *Functional Ecology* **6**: 469–475.

Wijnen B, Hunt EJ, Anzalone GC, Pearce JM. 2014. Open-source syringe pump library. *PLoS ONE* **9**: 1–8.

Zarebanadkouki M, Carminatti A. 2014. Reduced root water uptake after drying and rewetting. *Journal of Plant Nutrition and Soil Science* **177**: 227–236.

Zarebanadkouki M, Kim YX, Carminatti A. 2013. Where do roots take up water? Neutron radiography of water flow into the roots of transpiring plants growing in soil. *New Phytologist* **199**: 1034–1044.

Zwieniecki MA, Thompson MV, Holbrook NM. 2002. Understanding the hydraulics of porous pipes: tradeoffs between water uptake and root length utilization. *Journal of Plant Growth Regulation* **21**: 315–323.

Supporting Information

Additional Supporting Information may be found online in the Supporting Information tab for this article:

Fig. S1 Representative masked microCT images before processing and after processing for quantifying the volume occupied by empty porous spaces during hydration.

Fig. S2 Cartoon illustrating the setup of hydraulic measurements.

Fig. S3 Representative pressure–flow relationship of root with bark, soaked root, and root without bark treatments.

Fig. S4 Process of vessel refilling in excised woody roots documented using microCT scanning in the same position at different times.

Fig. S5 Advancing contact angle–surface of contact relationship.

Please note: Wiley Blackwell are not responsible for the content or functionality of any Supporting Information supplied by the authors. Any queries (other than missing material) should be directed to the *New Phytologist* Central Office.